Daptomycin forms cation- and size-selective pores in model membranes

TianHua Zhang[a], Jawad K. Muraih[b], Ben MacCormick[c], and Michael Palmer[ad]

[a]Department of Chemistry, University of Waterloo, Waterloo, Ontario, Canada

[b]Department of Chemistry, University of Al-Muthanna, Samawah, Al-Muthanna, Iraq

[c]BioMedica Diagnostics, Windsor, Nova Scotia, Canada

[d]Corresponding author. Email: mpalmer@uwaterloo.ca

Abstract

Daptomycin is a lipopeptide antibiotic that is used clinically to treat severe infections caused by Gram-positive bacteria. Its bactericidal action involves the calcium-dependent binding to membranes containing phosphatidylglycerol, followed by the formation of membrane-associated oligomers. Bacterial cells exposed to daptomycin undergo membrane depolarization, suggesting the formation of channels or pores in the target membranes. We here used a liposome model to detect and characterize the permeability properties of the daptomycin pores. The pores are selective for cations, with permeabilities being highest for Na^+, K^+, and other alkali metal ions. The permeability is approximately twice lower for Mg^{++}, and lower again for the organic cations choline and hexamethonium. Anions are excluded, as is the zwitterion cysteine. These observations account for the observed depolarization of bacterial cells by daptomycin and suggest that under typical in vivo conditions depolarization is mainly due to sodium influx.

Introduction

Daptomycin is the first clinically approved lipopeptide antibiotic; it has been available for injection under the trade name Cubicin® since 2003 [1]. It is used to treat severe infections caused by Gram-positive bacteria such as *Staphylococcus aureus* and *Enterococcus faecalis*, including strains that are resistant to β-lactam antibiotics and vancomycin [2, 3]. Daptomycin consists of a cyclic peptide moiety with 10 amino acids, from which the N-terminal three amino acids protrude; the N-terminus carries a decanoyl fatty acyl side chain (Figure 1). The antibiotic is extraribosomally synthesized by *Streptomyces roseosporus* [4, 5] and contains several non-standard amino acids.

Daptomycin acts at the bacterial membrane. Various molecular targets and action modes have been proposed, including the inhibition of peptidoglycan [6] or lipoteichoic acid synthesis [7]. However, the only effect consistently reported in studies from different laboratories consists in the depolarization of the bacterial cell membrane [8-11]. Concomitantly with membrane depolarization, bacterial cells lose the ability to accumulate amino acid substrates, while leaving glucose uptake intact, indicating a selective nature of the membrane permeability defect [9]. No membrane discontinuities have been observed by electron microscopy [12], also supporting the notion that the functional membrane lesion is discrete and small.

Based on precedent from other membrane-damaging peptides and proteins, it was proposed early on that daptomycin acts through the formation of oligomeric transmembrane pores [10]; however, experimental evidence was only obtained more recently. Using various fluorescently labeled, functionally active daptomycin derivatives, oligomerization was observed both on model liposomes and on bacterial membranes [13-15], and it was subsequently shown that oligomerization is required for antibacterial action [16]. The model liposomes used in those studies contained only phosphatidylcholine (PC), which is largely inert to daptomycin [13], and phosphatidylglycerol (PG), which was required to induce binding at physiologically relevant calcium concentration, as well as to trigger oligomer formation.

It is noteworthy that the abundance of phosphatidylglycerol in bacterial cell membranes is also a major determinant in the susceptibility of bacteria to daptomycin [17-19]. It was therefore of interest to determine whether the PC/PG liposome model also suffices to support the formation of the functional daptomycin pore, and if so, to characterize the pore's permeability properties. This study reports the corresponding experiments. The results show that daptomycin forms discrete pores on liposome membranes that are selective for cations of limited size.

Materials and methods

Preparation of indicator-loaded large unilamellar vesicles

1,2-Dimyristoyl-sn-glycero-3-phosphocholine (DMPC) and 1,2-Dimyristoyl-sn-glycero-3-phospho-rac-(1'-glycerol) (DMPG; both from Avanti Polar Lipids, Alabaster, AL, USA) were used to prepare the vesicles. Equimolar amounts of DMPC and DMPG were weighed into a round-bottom flask and dissolved in chloroform/methanol (3:1). The solvent mixture was then evaporated with nitrogen to produce a ipid film, which was further dried under vacuum for three hours and then dispersed in buffer. The resulting lipid suspension was extruded through a 100 nm polycarbonate filter 15 times, using a nitrogen-pressurized extruder to produce indicator-loaded large unilamellar liposomes [20].

The buffers used for dispersing the lipid film contained either pyranine or dithio-bis-nitrobenzoic acid (DTNB) as indicators for the permeabilization assays, and they varied in pH and salt composition as detailed in Table 1. Following polycarbonate membrane extrusion, the liposomes were subjected to gel filtration on a Bio-Rad P-6DG column (Bio-Rad, Richmond, CA, USA) in order to remove unentrapped indicator. The column buffers used in the gel filtration step matched those used for lipid film rehydration, except for the absence of pyranine or DTNB.

As indicated in Table 1, all loading buffers also contained 250 mM sucrose. This experimental detail was adopted from a previous study [21] and was found to improve the stability of the indicator-loaded liposomes.

Fluorescence measurements

With pyranine-loaded liposomes, time-based emission scans were acquired on a PTI QuantaMaster 4 system, the sample holder of which was thermostatted at 30 ºC. Liposome suspensions were diluted to a final concentration of 250 μM of total lipids into reaction buffer with 5mM $CaCl_2$. Daptomycin (Cubist), carbonyl cyanide m-chlorophenyl hydrazine (CCCP, Sigma), and valinomycin or gramicidin (Sigma) were added as indicated to final concentrations of 1 μM, 5 nM, 0.5 μM, and 10 nM, respectively, in order to initiate the reaction. The fluorescence emission at 510 nm was recorded for 5 minutes, with excitation at 460 nm. Triton X-100 was then added to a final concentration of 0.1%, followed by one more minute of recording; this was done in order to disrupt the liposomes and so establish the fluorescence intensity equivalent to 100% test solute permeation.

With cationic test solutes, the reaction buffer was similar to the corresponding liposome hydration buffer (see Table 1), but the concentration of the test solute was increased to 100 mM, and the pH value from 6.00 to 8.00. With the anionic test solute (Cl^-), the reaction buffer was similar to its hydration buffer, but choline chloride was added to 100 mM, and the pH value was lowered from 8.00 to 6.00. Using the intrinsic fluorescence of the kynurenine residue, we confirmed that daptomycin binds quantitatively to the model membranes under these experimental conditions (see Figure S1).

Spectrophotometric measurements

The permeation of thiols into the liposomes was measured through reduction of entrapped DTNB, which was measured by its absorption at 412 nm (ε=13,400 $M^{-1}cm^{-1}$). DTNB-loaded liposomes were diluted to a final concentration of 250 μM total lipids into the corresponding hydration buffer (Table 1) supplemented with 100 mM cysteine and 5 mM $CaCl_2$. 1 μM daptomycin was added to initiate the reaction.

Assessment of flow rate of different cations through daptomycin pores

To convert observed changes of pyranine fluorescence to permeation rates of cations, a calibration curve for pyranine fluorescence as a function of pH was recorded. 200 mL of

buffer (5 mM MES, 5 mM Tricine, 5 mM NaCl, 5 mM KCl, 250 mM sucrose, pH 6.00; the same as used for the liposome interior when testing cation permeation) containing 2 μM pyranine was titrated with 1 M NaOH, while measuring both the pyranine fluorescence intensity at 510 nm and the pH value after each successive addition. The measured curve was fitted with the empirical polynomial function:

$$y = ax + bx^{1/2} + cx^{1/3} + dx^{1/4}$$

The fitted function was then used as a calibration curve to convert the measured time-based fluorescence traces to changes in the intraliposomal proton concentration.

Results

Effect of daptomycin on cation permeability

The permeability of liposomes for cations was measured using a coupled fluorescence assay that is based on the pH-sensitive indicator pyranine, whose fluorescence increases with the pH as its phenolic OH group dissociates between pH 6 and 8.5 [21]. The experimental rationale, with potassium as an example, is illustrated in Figure 2. Dilution of the pyranine-loaded liposomes into the final reaction buffer containing 100 mM KCl at pH 8 creates two opposite ion concentration gradients across the liposome membrane: the K^+ concentration is higher outside, whereas the H^+ concentration is higher inside (Figure 2A). Addition of the proton ionophore CCCP alone to this system will cause little change to the pH within the liposomes, since the efflux of protons will very soon be restricted by the ensuing diffusion potential (Figure 2B). The internal pH will change significantly only after addition of daptomycin, if, and only if, daptomycin allows the influx of potassium ions. Both ion gradients will then dissipate, the interior pH will rise, and pyranine will dissociate and fluoresce (Figure 2C).

The findings obtained using this assay with different cations are illustrated in Figure 3. Panel A shows that the experiment works as expected with valinomycin, a potassium-specific ionophore. With potassium, but not with sodium, the combination of valinomycin and CCCP induces a rapid change that indicates swift dissipation of the proton gradient,

facilitated by exchange of protons and potassium ions across the membrane. CCCP alone does not induce an appreciable change in fluorescence, while valinomycin alone shows a minor one; it may be that valinomycin has a limited ability to translocate protons bound to it, as has been suggested earlier [22].

Figure 3B shows the same experiment with daptomycin instead of valinomycin. Again, only the combination of daptomycin and CCCP induces a major change of fluorescence, while either agent alone induces negligible changes in fluorescence. This indicates that daptomycin allows the influx of potassium ions. Also note that the rate of fluorescence change induced with daptomycin/CCCP was significantly smaller than with valinomycin/CCCP, which indicates that under the given experimental conditions the rate of fluorescence change was constrained by daptomycin and not by CCCP. This latter conclusion is further supported by the experiments shown in Figures S2 and S3.

Furthermore, when CCCP was added several minutes after daptomycin in order to allow lead time for daptomycin pore assembly before triggering ion gradient dissipation, the ensuing fluorescence traces were very similar to those obtained with simultaneous application (data not shown). This indicates that the rate of ion flux was not limited by the process of pore assembly, but rather by the permeability of the already assembled pores.

When significantly higher concentrations of daptomycin were employed together with CCCP, the rate of permeabilization increased, but there was also a notable increase in the rate of fluorescence change in the absence of CCCP (data not shown). This agrees with a previous study showing that, at higher concentrations, daptomycin destabilizes and induces fusion of lipid bilayers [23]. We therefore used a concentration of 1 μM throughout; this value is similar to minimal inhibitory concentrations in susceptible bacteria [24].

To further investigate the ion selectivity and functional size of the pores formed by daptomycin, the same experimental conditions were used on a series of cations (Figure 3C). The various metal ions, choline, and hexamethonium (N,N,N,N',N',N'-hexamethylhexane-1,6-diaminium) were all used as their respective chloride salts and at

the same molar concentrations. All metal ions produced a similar rate of fluorescence increase. Similar rates of permeabilization were also observed with lithium, rubidium, barium, and calcium (data not shown); however, calcium is also a cofactor of daptomycin activity, which might conceivably skew this measurement. Compared to the metal cations, choline and hexamethonium produced significantly lower increases in fluorescence intensity (Figure 3C). Both are organic cations and, in unhydrated form, are larger than the metal ions.

Effect of daptomycin on the permeability of anions

To determine whether daptomycin pores also allow the permeation of anions, the assay format was varied slightly. Pyranine-loaded liposomes with high internal pH (8.00) were diluted into a reaction buffer containing 100 mM choline chloride at low pH (6.00), creating H^+ and Cl^- gradients that point the same way. Choline has been shown above to be only slowly transported by daptomycin, whereas proton transport by CCCP is fast (compare Figure 3A); therefore, an influx of chloride should mostly be compensated by a simultaneous influx of protons, lowering the interior pH and causing the fluorescence to drop. This, however, was not observed; the fluorescence intensity was not significantly affected by the presence of daptomycin, with our without CCCP (Figure 4A). We conclude that daptomycin pores have no or low permeability for chloride ions.

Effect of daptomycin on the permeability of neutral solutes

DTNB (Ellman's reagent) is useful for detection of thiol groups in compounds such as cysteine. Its disulfide bond is readily cleaved by thiols to produce 2-nitro-5-thiobenzoate (NTB^-), which absorbs at 412 nm [25]. We here used it to test the permeation of thiols across daptomycin pores. In this experiment, DTNB-loaded liposomes were added to a solution containing 100 mM of thiol.

The experiment shown in Figure 4B depicts the findings obtained with cysteine. Absorption was measured every 2 minutes over a period of 10 minutes, which showed no significant change until 0.1% Triton X-100 was added. Addition of 1 μM daptomycin did not accelerate the reduction of DTNB (indeed it seemed to slightly delay it), indicating

that the daptomycin pore allows no or only slow passage of cysteine across the membrane.

Cysteine has a neutral net charge, but it is not uncharged. Two uncharged thiols, dithiothreitol (DTT) and 2-mercaptoethanol, were also tested. These molecules, however, were found to swiftly enter the liposomes and reduce DTNB even at lower concentrations and in the absence of daptomycin, so that no conclusion could be reached as to their ability to be transported by daptomycin pores.

These findings do not allow us clearly assess the ability of daptomycin to transport neutral solutes; cysteine transport may be limited either by lack of a positive charge or by its molecular size.

Estimation of the rate of ion flow across daptomycin pores

As illustrated in Figure 2, each proton that is to leave the liposome needs to be replaced by one (alkali metals and choline) or one half (magnesium and hexamethonium) cation that enters through a daptomycin pore. Therefore, a given decrease in the total (buffered and unbuffered) proton concentration corresponds to a proportional increase in the concentration of the test cation, and it is thus possible to estimate the rate of permeation through daptomycin pores from the rate of fluorescence change.

The relationship between pyranine fluorescence intensity and total proton concentration was determined empirically by titrating pyranine-containing cation hydration buffer with NaOH. The titration curve was mathematically fitted with an empirical polynomial function (Figure 5A), which was then used to convert the previously acquired fluorescence traces to changes of intravesicular cation concentrations (Figure 5B). The rates are highest for the alkali metal ions and lowest for magnesium and hexamethonium.

In Figure 5C, the rate of sodium transport during the first minute was approximated using a single-exponential fit. The parameters of this fit indicate an initial transport rate of 22 μM per second. To estimate the number of ions actually transported, we need to consider that the experiment observes the change in ion concentration only within the intraliposomal volume. Liposomes with 100 nm diameter and at a total lipid

concentration of 250 μM should enclose approximately 0.08% of the total volume. Therefore, an apparent ion transport rate of 22 μM/s converts to a liposomal entry of only 18 nM/s from the bulk volume. The daptomycin concentration is 1 μM; if all daptomycin molecules are indeed incorporated into functional pores, and each pore is an oligomer that consists of 7 or 8 subunits [14, 26], the average transport rate of each pore is approximately 0.12 sodium ions per second. While this is only a rough estimate, it is clear that ion transport by daptomycin is many orders of magnitude slower than those of typical cellular ion channels or of gramicidin, which transports upward of 10^6 ions per seond under similar conditions [27] (compare also Figure S2).

Discussion

In previous experiments, we have shown that daptomycin forms oligomers on the membranes of liposomes consisting of PC and PG, as well as on bacterial cells [13, 15]. These oligomers were subequently shown to contain approximately 7 subunits each [14] and to be involved in the bactericidal action of daptomycin [16]. We recently proposed a revised and more detailed model, in which the oligomer comprises eight subunits, with four each in the inner and the outer membrane leaflet [26].Earlier studies had established that daptomycin depolarizes the cell membranes of susceptible bacteria [8-10]. From the closely parallel observations obtained with the liposome model and with bacterial cells regarding oligomer formation, the question arose whether the functional daptomycin lesion could also be observed and characterized in the liposome model.

The findings reported here show that this is indeed the case. Daptomycin was found to permeabilize the liposome membranes in a cation-selective fashion. The rate of permeation was virtually the same for all alkali metal ions. It was approximately twice lower for magnesium, and lower again for the organic cations choline and hexamethonium, indicating that the pore also discriminates between different cations, most likely according to size.

When comparing the bare ions, without hydration shells, the two organic cations are much larger than all of the metal ions; both choline and hexamothonium contain tetramethylammonium as a moiety, which has an unhydrated diameter of 5.7 Å. In

contrast, when we take the hydration shells into account, magnesium at 8.6 Å exceeds the alkali metals and the organic ions, which are all close to 7 Å (all ionic diameters according to [28]). In membrane nanofiltration experiments [29], sodium and potassium have been found to be more permeant than magnesium and calcium, and it was proposed that nanopore permeation involved the partial shedding of hydration shells. Partial dehydration may also be involved in ion permeation across the the daptomycin pore. The organic cations bind their hydration shells most weakly [30]; nevertheless, they are less readily transported than the alkali metal ions, which suggests that daptomycin prefers ions with an effective radius below that of unhydrated choline or hexamethonium. Chloride, in both hydrated and unhydrated form, is very similar in diameter to potassium; therefore, its exclusion is apparently not caused by size but may be due to electrostatic repulsion between it and one of the several acidic residues on the daptomycin molecule. It seems likely that the pore is also permeable for protons; however, due to the very low free (as opposed to buffered) proton concentration at near neutral pH, this would not result in a rapid dissipation of transmembrane proton gradients and therefore would not be detected in our assay.

The observations reported here agree rather well with previous reports on the permeabilization of bacterial cells. Daptomycin depolarizes *Bacillus* cells and disrupts their uptake of amino acids, which is mostly driven by cation cotransport, but does not induce leakage of already accumulated amino acids [9]. The major cations that control the membrane potential are potassium and sodium. In an intact cell, the permeability is higher for potassium than for sodium, which creates a negative-inside membrane potential. Changing the permeability balance in favor of sodium will depolarize the membrane. This would occur with either sodium-selective channels or with non-selective pores such as those formed by daptomycin, which indeed reproducibly induces depolarization. Interestingly, one experimental study reported a short-lived yet distinct transient hyperpolarization, followed by depolarization [31]. The extracellular medium used in that study was low in sodium; in this situation, permeabilization for both sodium and potassium might produce a transient dominance of the strongly negative potassium

equilibrium potential, which would then collapse as the cytosol becomes depleted of potassium through continued leakage.

A quantitative estimation of the rate of ion transport for a single daptomycin pore indicated that this rate is several orders of magnitude lower than that of gramicidin, another peptide antibiotic that permeabilizes membranes for cations. It must be noted that the transport rate obtained here for daptomycin is an average value; while it might indeed apply to each of the functional pores in the ensemble, it is also possible that only a small fraction of all daptomycin oligomers form functional pores, with correspondingly greater permeability, or that the pores alternate between closed and open states, with the latter only prevailing during a small fraction of the time. While the conductivity properties of the individual daptomycin pore must be determined in future experiments, the low average conductivity, compared with a dedicated channel former such as gramicidin, might suggest that pore-formation may be only one of several aspects of daptomycin's bactericidal action. It should, however, be noted that no additional action mode has been biochemically substantiated [11]. Moreover, liposome permeabilization is readily observed with daptomycin concentrations equivalent to typical MIC values [10], even though the ratio of daptomycin molecules to membrane lipids is lower in a liposome expe than in a bacterial culture freshly inoculated for MIC measurement; this supports the notion that membrane permeabilization is relevant to antibacterial activity.

In sum, our study shows that a very simple artificial membrane model suffices to elicit and characterize the pore-forming activity of daptomycin. The only lipid specifically required for pore formation in our model is PG. A key role for PG in vivo is consistent with several studies on the causation of bacterial resistance to daptomycin [17-19]. The availability of a simple yet sufficient liposome model for daptomycin pore formation should be useful in further characterizing the structure and action mode of daptomycin, as well as the molecular basis of bacterial resistance.

Acknowledgements

This study was supported through a CHRP grant to M. Palmer by NSERC and CIHR. We thank two anonymous reviewers for valuable suggestions and important criticisms.

Table 1

Buffers and indicators used to detect membrane permeabilization toward different solutes. The indicators were dissolved in the corresponding hydration buffer, and the solution was then used to rehydrate PC/PG lipid films. After extrusion of the lipid dispersion through polycarbonate membranes, unentrapped indicator was removed by gel filtration using the corresponding hydration buffer. In experiments with anionic or cationic test solutes, pH gradients were established by diluting the liposome samples into reaction buffers with different pH. Pyranine (8-hydroxypyrene-1,3,6-trisulfonic acid) and DTNB (5,5'-dithiobis-(2-nitrobenzoic acid)) were obtained from Sigma.

Test solutes	**Hydration buffer**	**Entrapped indicator**	**pH value**
Cations	5 mM MES, 5 mM Tricine, 5 mM NaCl, 5 mM KCl, 250 mM Sucrose	5 mM pyranine	6.00
Anions	5 mM MES, 5 mM Tricine, 5 mM NaCl, 5 mM KCl, 250 mM Sucrose	5 mM pyranine	8.00
Neutral solutes (thiols)	20 mM HEPES, 150 mM NaCl, 250 mM Sucrose	5 mM DTNB	7.00

Legends to Figures

Figure 1. Schematic of the structure of daptomycin. Arrows indicate amide bonds, except between kynurenine and threonine, where an ester bond between the carboxyl group of kynurenine and the side chain hydroxyl group of threonine closes the ring.

Figure 2. Schematic representation of the pyranine-based liposome permeabilization assay, using K^+ ions as an example. Liposomes loaded with pyranine were diluted into the final reaction buffer to create two opposite ion concentration gradients across the membrane (A). Application of the protonophor CCCP alone will create a diffusion potential, which will prevent a major efflux of protons (B). If daptomycin is added also and allows K^+ ions to enter, both ion gradients can dissipate, the pH in the liposome will rise, and pyranine fluorescence will increase (C).

Figure 3. Time-based fluorescence traces of pyranine-loaded liposomes after exposure to different test solutes and permeabilizing agents, which were added at t=0. The interior pH was 6 and the exterior pH was 8. Test solutes added to the exterior buffer at 100 mM were KCl in B, and otherwise as indicated; "hexa" in C and D is hexamethonium. After 300 seconds, the samples were solubilized with Triton-X100, and the fluorescence monitored for another minute. The fluorescence intensity observed after Triton solubilization was used to normalize each fluorescence trace. **A:** Valinomycin (val., 0.5 μM) with CCCP (5 nM) permeabilize liposomes for potassium but not sodium. **B:** Daptomycin (1 μM) plus CCCP (5 nM) also causes permeabilization for potassium. **C:** Permeabilization traces obtained with both daptomycin and CCCP present, after subtraction of the traces obtained with CCCP only. **D:** Averages and standard deviations of fluorescence intensities after 300 seconds of incubation, for 3 or 4 independent experiments performed as in C ("chol." is choline).

Figure 4. Absence of liposome permeabilization toward chloride (A) and cysteine (B). **A:** Pyranine-loaded liposomes with an interior pH of 6 were diluted 100 mM choline chloride, pH 8, and CCCP (5 nM) and daptomycin (1 μM) were added at t=0.

Permeabilization for chloride should have resulted in an accelerated dissipation of the pH gradient and concomitant drop in pyranine fluorescence. The experiment shown is one of 4 independent ones and is representative. **B:** Time course of reduction of DTNB entrapped in liposomes by 100 mM cysteine added to the outside, in the absence and presence of daptomycin (1 μM). Reduction of DTNB results in an increase of the absorption at 412 nm. After the last reading at 10 minutes, samples were solubilized with Triton-X100, resulting in immediate complete DTNB reduction. Error bars are standard deviations from three independent experiments. Daptomycin does not increase in the permeation of cysteine into the liposomes.

Figure 5. Conversion of observed pyranine fluorescence changes to cation flow rates. A calibration curve relating total (buffered and unbuffered) proton concentration to pyranine fluorescence intensity was obtained by titrating a solution matching the liposome interior with NaOH (A). A polynomical function was fitted to the measured values. In panel B, the polynomial function obtained in A was applied to the raw fluorescence traces shown in Figure 3C in order to transform them to ion fluxes. The flow rates for hexamethonium and Mg^{++} were then divided by 2, as each of these cations is exchanged for 2 protons. In C, an exponential function was fitted to the transport curve for sodium in order to estimate the initial transport rate (see text for further details).

References

[1] Eisenstein, B.I., Oleson, F.B.J. and Baltz, R.H. Daptomycin: from the mountain to the clinic, with essential help from Francis Tally, MD, Clin Infect Dis *50 Suppl 1* (2010) S10-5.

[2] Tally, F.P. and DeBruin, M.F. Development of daptomycin for gram-positive infections, J Antimicrob Chemother *46* (2000) 523-526.

[3] Steenbergen, J.N., Alder, J., Thorne, G.M. and Tally, F.P. Daptomycin: a lipopeptide antibiotic for the treatment of serious Gram-positive infections, J Antimicrob Chemother *55* (2005) 283-288.

[4] Debono, M., Barnhart, M., Carrell, C.B., Hoffmann, J.A., Occolowitz, J.L., Abbott, B.J., Fukuda, D.S., Hamill, R.L., Biemann, K. and Herlihy, W.C. A21978C, a complex of new acidic peptide antibiotics: isolation, chemistry, and mass spectral structure elucidation, J Antibiot (Tokyo) *40* (1987) 761-777.

[5] Baltz, R.H. Biosynthesis and genetic engineering of lipopeptide antibiotics related to daptomycin, Curr Top Med Chem *8* (2008) 618-638.

[6] Mengin-Lecreulx, D., Allen, N.E., Hobbs, J.N. and van Heijenoort, J. Inhibition of peptidoglycan biosynthesis in Bacillus megaterium by daptomycin, FEMS Microbiol Lett *57* (1990) 245-248.

[7] Canepari, P., Boaretti, M., Lleó, M.M. and Satta, G. Lipoteichoic acid as a new target for activity of antibiotics: mode of action of daptomycin (LY146032), Antimicrob Agents Chemother *34* (1990) 1220-1226.

[8] Alborn, W.E.J., Allen, N.E. and Preston, D.A. Daptomycin disrupts membrane potential in growing Staphylococcus aureus, Antimicrob Agents Chemother *35* (1991) 2282-2287.

[9] Allen, N.E., Alborn, W.E.J. and Hobbs, J.N.J. Inhibition of membrane potential-dependent amino acid transport by daptomycin, Antimicrob Agents Chemother *35* (1991) 2639-2642.

[10] Silverman, J.A., Perlmutter, N.G. and Shapiro, H.M. Correlation of daptomycin bactericidal activity and membrane depolarization in Staphylococcus aureus, Antimicrob Agents Chemother *47* (2003) 2538-2544.

[11] Rubinchik, E., Schneider, T., Elliott, M., Scott, W.R.P., Pan, J., Anklin, C., Yang, H., Dugourd, D., Müller, A., Gries, K., Straus, S.K., Sahl, H.G. and Hancock, R.E.W. Mechanism of action and limited cross-resistance of new lipopeptide MX-2401, Antimicrob Agents Chemother *55* (2011) 2743-2754.

[12] Cotroneo, N., Harris, R., Perlmutter, N., Beveridge, T. and Silverman, J.A. Daptomycin exerts bactericidal activity without lysis of Staphylococcus aureus, Antimicrob Agents Chemother *52* (2008) 2223-2225.

[13] Muraih, J.K., Pearson, A., Silverman, J. and Palmer, M. Oligomerization of daptomycin on membranes, Biochim Biophys Acta *1808* (2011) 1154-1160.

[14] Muraih, J.K. and Palmer, M. Estimation of the subunit stoichiometry of the membrane-associated daptomycin oligomer by FRET, Biochim Biophys Acta *1818* (2012) 1642-1647.

[15] Muraih, J.K., Harris, J., Taylor, S.D. and Palmer, M. Characterization of daptomycin oligomerization with perylene excimer fluorescence: stoichiometric binding of phosphatidylglycerol triggers oligomer formation, Biochim Biophys Acta *1818* (2012) 673-678.

[16] Zhang, T., Muraih, J.K., Mintzer, E., Tishbi, N., Desert, C., Silverman, J., Taylor, S. and Palmer, M. Mutual inhibition through hybrid oligomer formation of daptomycin and the semisynthetic lipopeptide antibiotic CB-182,462, Biochim Biophys Acta *1828* (2013) 302-308.

[17] Baltz, R.H. Daptomycin: mechanisms of action and resistance, and biosynthetic engineering, Curr Opin Chem Biol *13* (2009) 144-151.

[18] Friedman, L., Alder, J.D. and Silverman, J.A. Genetic changes that correlate with reduced susceptibility to daptomycin in Staphylococcus aureus, Antimicrob Agents Chemother *50* (2006) 2137-2145.

[19] Hachmann, A., Sevim, E., Gaballa, A., Popham, D.L., Antelmann, H. and Helmann, J.D. Reduction in membrane phosphatidylglycerol content leads to daptomycin resistance in Bacillus subtilis, Antimicrob Agents Chemother *55* (2011) 4326-4337.

[20] Mayer, L.D., Hope, M.J. and Cullis, P.R. Vesicles of variable sizes produced by a rapid extrusion procedure, Biochim Biophys Acta *858* (1986) 161-168.

[21] Clement, N.R. and Gould, J.M. Pyranine (8-hydroxy-1,3,6-pyrenetrisulfonate) as a probe of internal aqueous hydrogen ion concentration in phospholipid vesicles, Biochemistry *20* (1981) 1534-1538.

[22] Kríz, J., Dybal, J. and Makrlík, E. Valinomycin-proton interaction in low-polarity media, Biopolymers *82* (2006) 536-548.

[23] Jung, D., Powers, J.P., Straus, S.K. and Hancock, R.E.W. Lipid-specific binding of the calcium-dependent antibiotic daptomycin leads to changes in lipid polymorphism of model membranes., Chem Phys Lipids *154* (2008) 120-128.

[24] Laganas, V., Alder, J. and Silverman, J.A. In vitro bactericidal activities of daptomycin against Staphylococcus aureus and Enterococcus faecalis are not mediated by inhibition of lipoteichoic acid biosynthesis, Antimicrob Agents Chemother *47* (2003) 2682-2684.

[25] Ellman, G.L. Tissue sulfhydryl groups, Arch Biochem Biophys *82* (1959) 70-77.

[26] Zhang, T., Muraih, J.K., Tishbi, N., Herskowitz, J., Victor, R.L., Silverman, J., Uwumarenogie, S., Taylor, S.D., Palmer, M. and Mintzer, E. Cardiolipin prevents membrane translocation and permeabilization by daptomycin, J Biol Chem *in press* (2014) .

[27] Finkelstein, A. and Andersen, O.S. The gramicidin A channel: a review of its permeability characteristics with special reference to the single-file aspect of transport, J Membr Biol *59* (1981) 155-171.

[28] Volkov, A.G., Paula, S. and Deamer, D.W. Two mechanisms of permeation of small neutral molecules and hydrated ions across phospholipid bilayers, Bioelectrochem Bioenergetics *42* (1997) 153-160.

[29] Tansel, B., Sager, J., Rector, T., Garland, J., Strayer, R.F., Levine, L., Roberts, M., Hummerick, M. and Bauer, J. Significance of hydrated radius and hydration shells on ionic permeability during nanofiltration in dead end and cross flow modes, Separation and Purification Technology *51* (2006) 40-47.

[30] Anslyn, E.V. and Dougherty, D.A. (2006). Modern Physical Organic Chemistry, Edition (University Science Books).

[31] Mascio, C., Townsend, K., Cotroneo, N. and Silverman, J. (2009). Microbiological Characterization of a Novel Lipopeptide Antibiotic with Activity in Pulmonary Surfactant (49th Interscience Conference on Antimicrobial Agents and Chemotherapy, September 12–15, 2009, San Francisco, CA, American Society For Microbiology, Washington, D. C.).

Figure 1

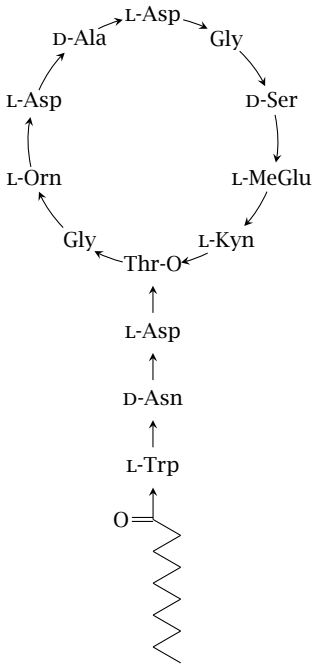

Figure 2

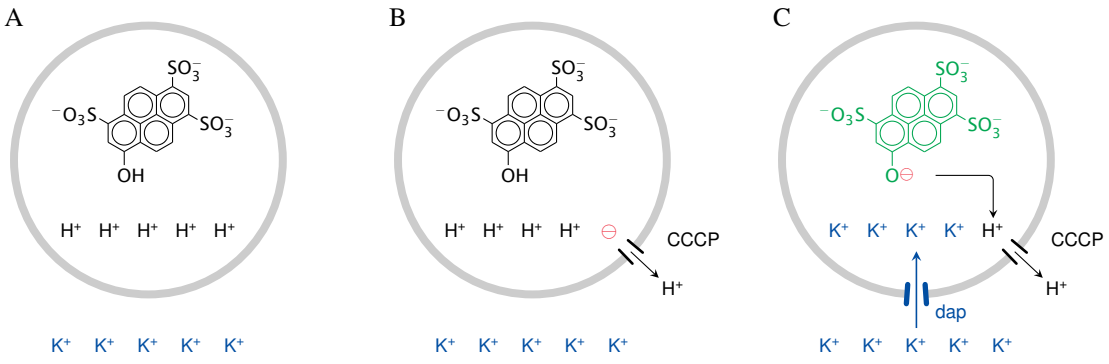

Figure 3

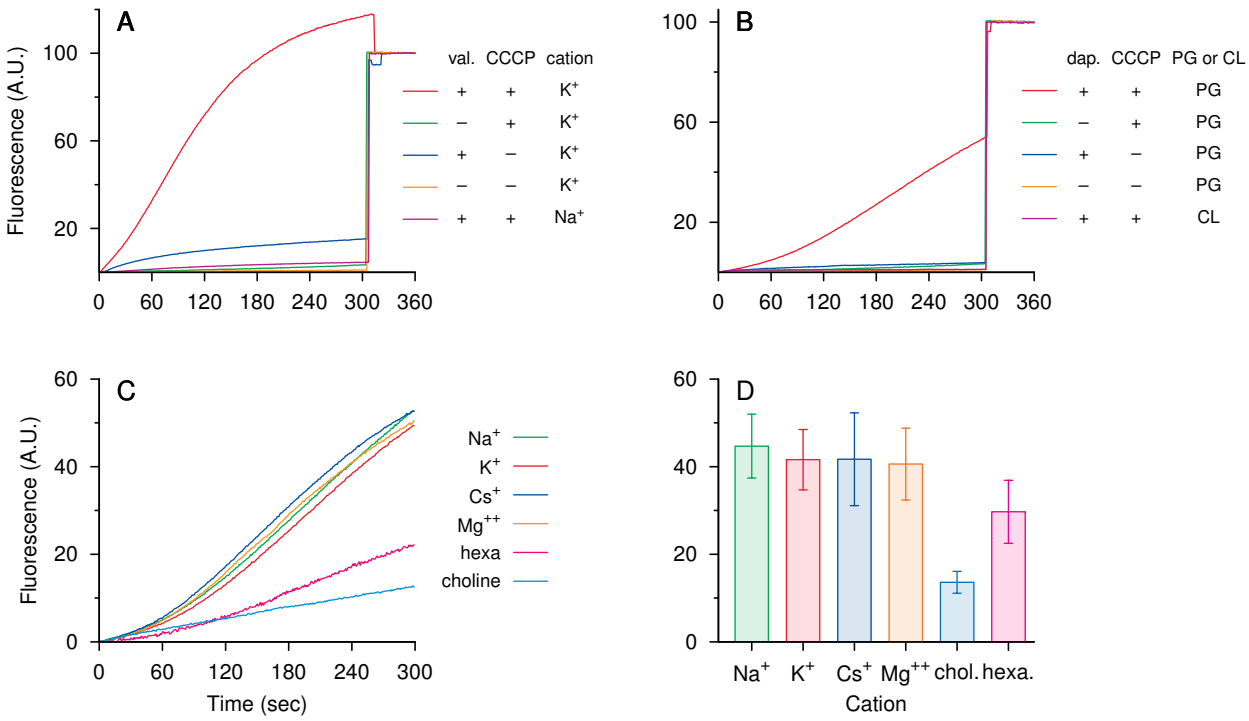

Figure 4

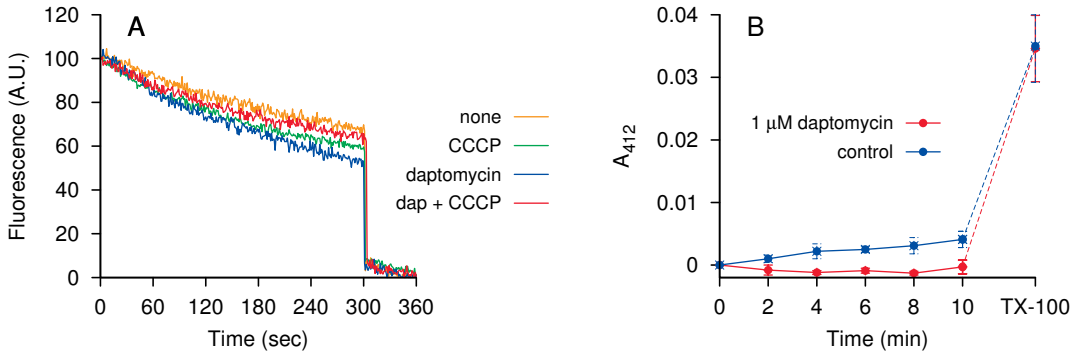

Figure 5

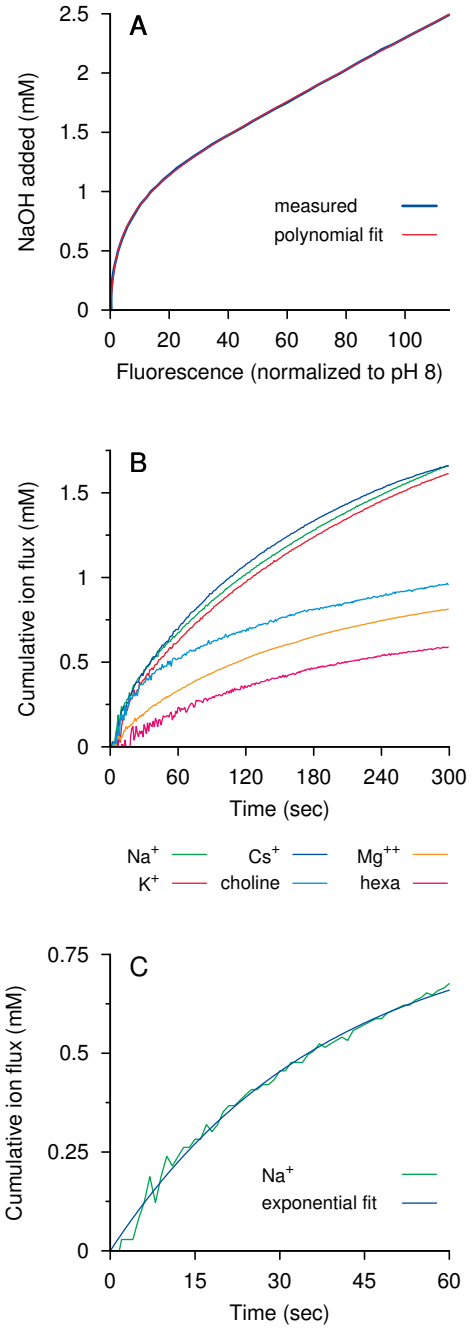
A
NaOH added (mM)
2.5
2
1.5
1
0.5
0
0
20
40
60
80
100
Fluorescence (normalized to pH 8)
measured
polynomial fit
B
Cumulative ion flux (mM)
1.5
1
0.5
0
0
60
120
180
240
300
Time (sec)
Na+
Cs+
Mg++
K+
choline
hexa
C
Cumulative ion flux (mM)
0.75
0.5
0.25
0
0
15
30
45
60
Time (sec)
Na+
exponential fit

Graphical abstract